Reprinted from

JAPANESE JOURNAL OF
APPLIED
PHYSICS

REGULAR PAPER

Large Remanent Polarization in Sm-Substituted $BiFeO_3$ Thin Film Formed by Chemical Solution Deposition

Zhiyong Zhong, Yoshihiro Sugiyama, and Hiroshi Ishiwara

Jpn. J. Appl. Phys. **49** (2010) 041502

Japanese Journal of Applied Physics **49** (2010) 041502 **REGULAR PAPER**

Large Remanent Polarization in Sm-Substituted $BiFeO_3$ Thin Film Formed by Chemical Solution Deposition

Zhiyong Zhong, Yoshihiro Sugiyama[1], and Hiroshi Ishiwara*

Interdisciplinary Graduate School of Science and Engineering, Tokyo Institute of Technology, 4259 Nagatsuta, Midori-ku, Yokohama 226-8503, Japan
[1]*Fujitsu Laboratories, Ltd., 10-1 Morinosato-Wakamiya, Atsugi, Kanagawa 243-0197, Japan*

Received August 8, 2009; revised December 2, 2009; accepted January 21, 2010; published online April 20, 2010

$Bi_{1-x}Sm_xFeO_3$ ($x = 0-0.15$) (BSFO) thin films were formed on $Pt/Ti/SiO_2/Si(100)$ substrates by chemical solution deposition. The spin-coated, dried, and prefired thin films were finally crystallized at 500 °C in air and in N_2. It was found that Sm-substitution for Bi in $BiFeO_3$ increased the grain size and the leakage current density. The optimal concentration for improving remanent polarization (P_r) was characterized to be 5 at. %. In 10 and 15 at. % BSFO films, incorporation of Sm atoms was found to be excess, leading to degradation of ferroelectric properties. The P_r and coercive electric field values in 5 at. % BSFO film measured at electric field of 1.5 MV/cm and frequency of 25 kHz were 82 μC/cm^2 and 0.35 MV/cm, respectively. In addition, the minimal coercive electric voltage of 7.5 V was achieved in a 126-nm-thick 7.5 at. % Sm-substituted BFO film.

DOI: 10.1143/JJAP.49.041502

1. Introduction

$BiFeO_3$ (BFO) is one of the prominent multiferroic materials which simultaneously show ferroelectricity and ferromagnetism because of its high Curie temperature (T_C) of ~850 °C and high Neel temperature (T_N) of ~370 °C.[1] And it has stimulated a great deal of scientific interests due to its potential applications for data storage, transducer, and actuators.[2–4] The lead-free ferroelectric BFO is a promising candidate to substitute for the currently used lead zirconate titanate (PZT) in one transistor–one capacitor (1T1C)-type ferroelectric random access memories (FeRAMs) due to its good ferroelectric and environmentally friendly properties. However, there is no applicable BFO-based composite reported to be used for fabrication of FeRAMs thanks to the unsolved challenges such as poor resistivity, large coercive voltage, and poor fatigue endurance. Up to now, a variety of research work has been conducted to further improve the ferroelectric and leakage current properties of BFO films using site engineering methods, such as substitution of Ti, Mn, Ni, Cr, and Cu for Fe atoms, or substitution of La, Nd, and Sm for Bi atoms.[5–10] Among them, a large remanent polarization (P_r) of 82 μC/cm^2 have been reported in Mn-substituted BFO films.[11]

Later on, characteristics of Sm-substituted BFO (BSFO) films were studied by several groups. In 2006, Yuan *et al.* reported a triclinic structure with $P1$ space group in a single-phase bulk $Bi_{0.875}Sm_{0.125}FeO_3$ multiferroic ceramics rather than the typical $R3c$ rhombohedral structure in BFO crystal, and ferroelectric behavior was also observed in that ceramics showing a P_r of 15 μC/cm^2.[15] In 2008, Fujino *et al.*[12] reported in pulse-laser-deposited (PLD) films that the morphotropic phase underwent substantial change in the out-of-plane lattice constant through transition from rhombohedral BFO to orthorhombic $Bi_{1-x}Sm_xFeO_3$ ($x \geq 0.13$) due to the difference of ionic radii between Bi^{3+} (1.365 Å) and Sm^{3+} (1.24 Å).[16] Especially, the antiferroelectric behavior was observed in the $Bi_{0.84}Sm_{0.16}FeO_3$ film.

In 2009, the detailed investigation on epitaxial BSFO films has been reported by the same group in succession.[16] On the basis of experimental results measured by high-resolution transmission electron microscopy and selected-area diffraction pattern, they proposed the transition from ferroelectric to antiferroelectric phases induced by morphotropic phase transition as Sm-substitution ratio varied in the BSFO films. Those interesting results intrigue us to speculate whether or not Sm-substitution can be used to enhance the ferroelectric properties of the polycrystalline BSFO film formed via chemical solution deposition (CSD), since ferroelectric properties in perovskite structures mainly result from the lattice distortion based on the Goldschmidt tolerance factor.

2. Experimental Procedure

The metalorganic decomposition (MOD) BSFO solutions with various Sm ratios were prepared by mixing bismuth(III) 2-ethylhexanoate [$Bi(OCOCH(C_2H_5)C_4H_9)$], samarium(III) 2-ethylhexanoate [$Sm(OCOCH(C_2H_5)C_4H_9)$], and iron(III) acetylacetonate [$Fe(C_5H_7O_2)_3$] and by diluting them with toluene. They were then spin-coated on $Pt/Ti/SiO_2/Si(100)$ substrates at 3000 rpm for 30 s, dried at 240 °C for 3 min, and prefired at 350 °C for 10 min in air. This process was repeated 15 times to form films with thicknesses of 450 nm, then the samples were crystallized in N_2 or in air at 500 °C. Next, Pt top electrodes of 3.14×10^{-4} cm^2 were deposited by e-beam evaporation through a shadow mask. Finally, those samples were post-annealed to improve the interfacial properties between the top electrodes and the films using the same parameters as those in the crystallization annealing.

The crystalline structure of these films was studied using a multipurpose X-ray diffractometer (Philips X'Pert-Pro MPD). The surface morphology of the ferroelectric films was examined by scanning electron microscopy (SEM). The ferroelectric and electrical properties of BSFO capacitors were measured at room temperature (RT) using a ferroelectric test system (Toyo) and a precision semiconductor parameter analyzer (HP 4156C).

3. Results and Discussion

Figure 1 shows X-ray diffraction (XRD) patterns of BSFO films with 0, 5, 10, and 15 at. % Sm-substitution. Different from the epitaxial BSFO film, only the rhombohedral phase could be seen in each BSFO film, i.e., substitution of Sm for Bi in BFO films did not lead to a morphotropic phase

*E-mail address: ishiwara.h.aa@m.titech.ac.jp

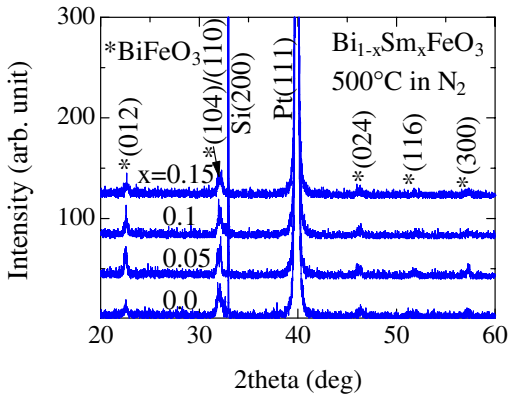

Fig. 1. (Color online) XRD patterns of 0, 5, 10, and 15 at. % BFSO films crystallized at 500 °C in N_2.

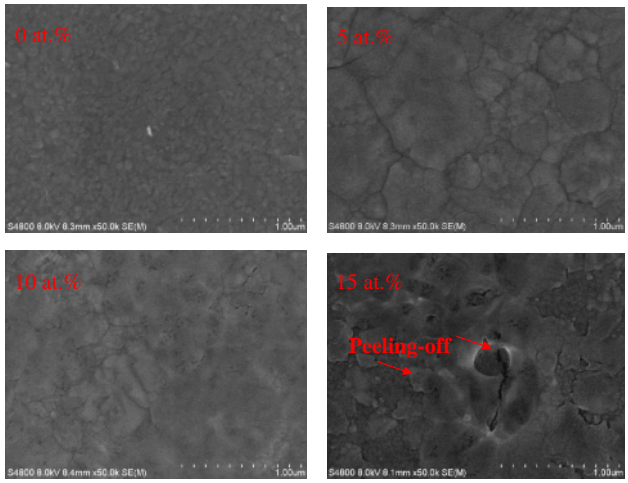

Fig. 2. (Color online) Surface micrographs for 0, 5, 10, and 15 at. % BSFO films crystallized at 500 °C in N_2 (for the 5 at. % BSFO film, the temperature was increased to 550 °C to see clearer grain boundaries).

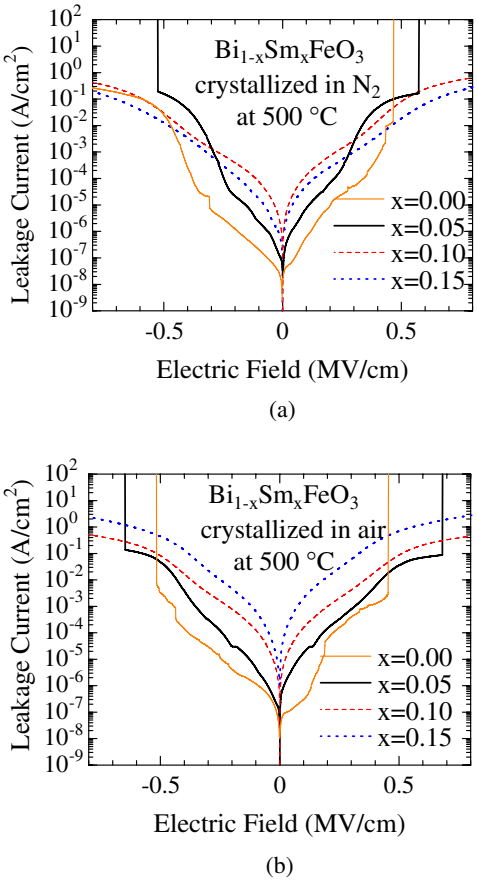

Fig. 3. (Color online) Leakage current characteristics of BSFO films crystallized at 500 °C in (a) N_2 and (b) air with 0, 5, 10, and 15 at. % Sm-substitution.

transition in these polycrystalline films. Instead, as shown in Fig. 2, the observed grain size was greatly increased in the 5 at. % BSFO film in comparison with the pure BFO film, whereas, some peeling-off phenomena were found on the surface of the 15 at. % BSFO film. The peeling-off might be caused by the over-doping of Sm, due to which P_r was found to be severely decreased in the high frequency measurement. The detailed discussion on it will be conducted later.

Figure 3(a) shows leakage current characteristics of the BSFO films crystallized at 500 °C in N_2 with 0, 5, 10, and 15 at. % Sm-substitution. It can be seen that leakage current density (at electric fields lower than 0.3 MV/cm) increases with Sm-substitution ratio up to 10 at. %, whereas it decreases in the 15 at. % BSFO film. As is well known, all analyses on leakage mechanisms such as ohmic conduction and space-charge-limited conduction (SCLC) are followed with an assumption that the film bulk is homogeneous in electric properties. On the other hand, there is another theory on leakage mechanism which involves the effects of grain boundaries. On the basis of grain-boundary-limited conduction (GBLC) theory, the increased leakage current density is considered to be related to the large grain size.[13] In the GBLC theory, it is expatiated that some potential barriers can be formed along the grain boundaries due to the abundance of charge traps, causing the higher resistivity at the grain boundaries than in the grains. In the fine-grained film which has high density of grain boundaries, the grain boundaries give rise to an increase of potential barriers, resulting in high resistivity. Thus, the increase of leakage current density in low electric field region can be explained by the increased grain size. Similar experimental results have also been obtained in $Pb(Zr_{0.45}Ti_{0.55})O_3$ thin films.[14]

The improved breakdown field in 10 and 15 at. % BSFO films might be explained by the SCLC in solids proposed by Rose.[17] In any insulating films with traps, there are at least two types of mechanisms competing to dominate the conduction: ohmic and SCLC. In the insulating film with more free electrons in the conduction band, the ohmic conduction can be maintained more easily even at a higher electric field. It is worth stressing that ohmic conduction does not involve any electron traps so that it is relatively stable as electric field increases. On the other hand, in the insulating film with less free electrons, the conduction mechanism can be transformed into SCLC even at a very low electric field due to the lack of free electrons in the conduction band. As the transformation is triggered at a certain electric field, the electron traps in the film should be filled up first, leading to a great number of electrons at the cathode injected into the insulator in a short time. This injection process is fatal for the Pt electrodes to be damaged. That is the possible reason for low breakdown filed for the 0 and 5 at. % BSFO films. Similar phenomena were found in Mn-substituted BFO

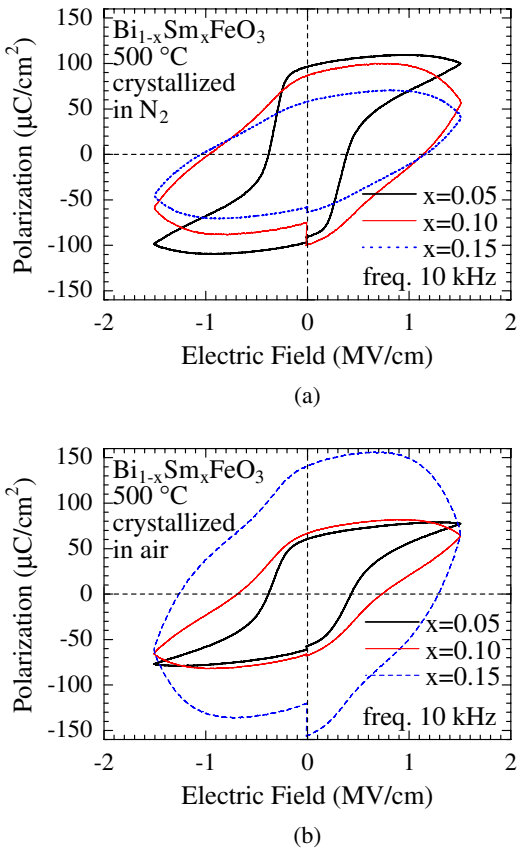

Fig. 4. (Color online) Comparison of hysteresis loops of 5, 10, and 15 at. % BSFO films crystallized at 500 °C in (a) N_2 and (b) air.

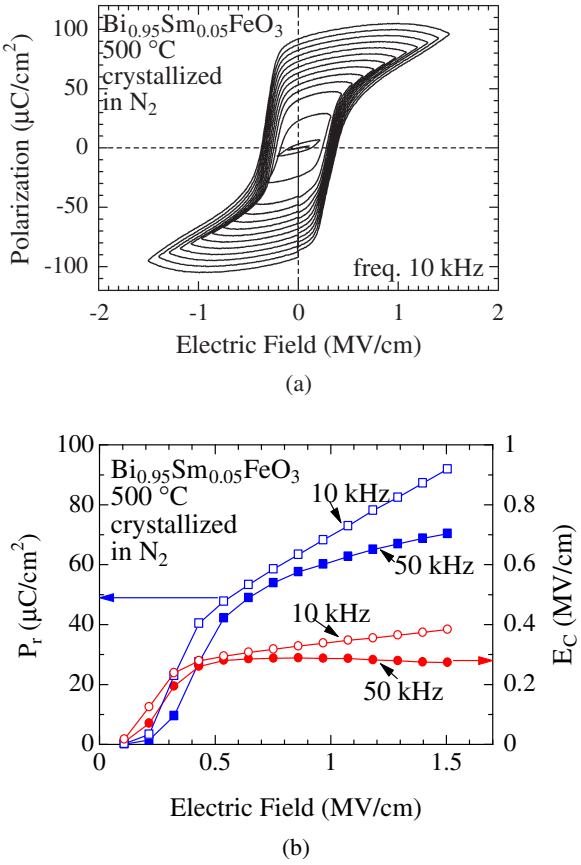

Fig. 5. (Color online) (a) Sweeping hysteresis loops of 5 at. % BSFO film crystallized at 500 °C in N_2, and (b) applied electric field dependences of P_r and E_c measured at 10 and 50 kHz.

films.[18] However, the higher breakdown field in BSFO films makes it possible to fabricate thinner films for achieving low voltage operation of FeRAMs.

In Fig. 3(b), the batch of BSFO films crystallized in air showed regular increase of both leakage current density and electrical breakdown corresponding to the increasing Sm-substitution ratio. It is well known that annealing atmosphere has an impact on formation of oxygen vacancies in BFO films. In 0 and 5 at. % BSFO films crystallized in air, the relatively lower leakage current densities are attributed to the partial oxygen pressure by which the oxygen vacancies can be partially compensated during the crystallization process. Nevertheless, the opposite results were obtained in 10 and 15 at. % BSFO films due to the over-doping ratio. It is interesting to find out that the leakage current level is closely related to the shapes of hysteresis loops.

Polarization vs electric field (P–E) characteristics of BSFO films crystallized at 500 °C in air and in N_2 are shown in Figs. 4(a) and 4(b), respectively in which their hysteresis loops were measured at a frequency of 10 kHz. It is worth stressing that the hysteresis loops in 10 and 15 at. % BSFO films are all rounded in their shape. It was also found from the frequency-dependent measurement of P_r that larger leakage current components were included in the hysteresis loops of 10 and 15 at. % BSFO films, and the results are consistent with the higher leakage current densities in them (Fig. 3). The worsened ferroelectric properties in 10 and 15 at. % BSFO films might be caused by the over-doping of Sm, which implies substitution of Sm atoms is limited to less than 10 at. %. The remaining Sm atoms might exist in the form of secondary non-ferroelectric phases so that the observed P_r values are decreased in the film capacitors. We conclude from these results that the 5 at. % BSFO film shows the best ferroelectric properties. However, it is speculated that the practical doping limit depends on the fabrication processes.

Figure 5(a) shows sweeping hysteresis loops from low to high electric field measured at 10 kHz. The regular-shaped hysteresis loops without any distortion caused by the antiferroelectric and/or domain pinning phenomena were obtained even at a very low electric field. Figure 5(b) shows the comparison of P_r and E_c measured at 10 and 50 kHz. The saturation of P_r and E_c starts from 0.5 MV/cm and a large P_r of 90 μC/cm^2 and E_c of 0.4 MV/cm was measured at 1.5 MV/cm and 10 kHz. The large E_c in the BSFO film is considered to be caused by the relatively high density of electron traps, due to which the BSFO film acts as an electron reservoir during the electric measurement. That is, when a voltage is applied for switching the domains, a lot of electrons are simultaneously injected into the film from the cathode. Then, as the applied field changes its direction and starts increasing towards E_c, the reserved electrons at the traps will partially neutralize the electric field. This means that a larger voltage is needed for switching the domains completely.

This explanation is verified by the slightly reduced E_c (0.3 MV/cm) measured at 50 kHz under which the injected charges are effectively reduced by a short period of applied voltage. The same tendency that E_c is decreased by increasing the measuring frequency was also observed for 10 and 15 at. % BSFO films. Particularly for the films

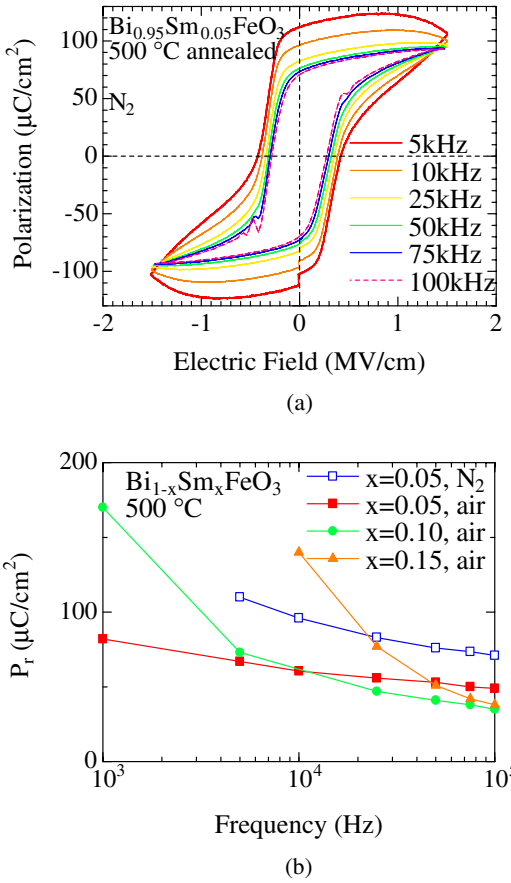

Fig. 6. (Color online) (a) Frequency-dependent hysteresis loops of 5 at. % BSFO film crystallized at 500 °C in N_2, and (b) frequency-dependent P_r values for the related samples crystallized in N_2 and air.

crystallized in air, the change rate of E_c to frequency is even greater than that in 5 at. % BSFO film due to the high leakage current level that ensures serious charge injection.

Figure 6(a) shows hysteresis loops for a 5 at. % BSFO film crystallized at 500 °C in N_2 which were measured at 1.5 MV/cm at various frequencies. As shown in the figure, P_r values decreased from 112 to 71 μC/cm^2 by changing the frequency from 5 to 100 kHz, but they are virtually free of frequency variation when frequency is higher than 25 kHz. Figure 6(b) shows the comparison of P_r values for 5, 10, and 15 at. % BSFO films crystallized at 500 °C in air and in N_2. We conclude from these results that the apparent P_r values are much enhanced by the large leakage current component in 10 and 15 at. % BSFO films, particularly at low frequencies. On the contrary, the effect of leakage current is negligible in the 5 at. % BSFO film crystallized in N_2 when the measurement frequency is higher than 25 kHz and thus large P_r of 82 μC/cm^2 was considered to be the real one.

Since it was figured out that electric breakdown field was improved by Sm-substitution, we conducted another experiment for achieving low coercive voltage for BSFO films, in which a batch of 7.5 at. % BSFO films with a variation of thickness was formed to balance the breakdown field and P_r. Their hysteresis loops were measured successfully in a 126 nm-thick film, and the minimal coercive voltage was measured to be 7.5 V as shown in Fig. 7.

4. Conclusions

In conclusion, Sm-substitution for Bi in BFO increased the grain size, then resulting in an increase of leakage current density at low electric fields, but it also increased electric breakdown field. The optimal Sm concentration for improving P_r was characterized to be 5 at. %. In the 5 at. % film, a P_r value as large as 82 μC/cm^2 was obtained with a coercive electric field (E_c) of 0.35 MV/cm at 1.5 MV/cm and 25 kHz. The minimal coercive voltage for the BSFO film was measured to be 7.5 V in a 126-nm-thick film with 7.5 at. % Sm-substitution.

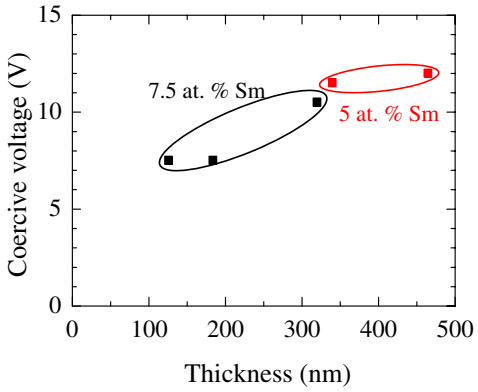

Fig. 7. (Color online) Thickness-dependent coercive voltage values for 5 and 7.5 at. % BSFO films measured at 100 kHz.

Acknowledgements

A part of this work is supported by the Japan Society for the Promotion of Science (JSPS) within the framework of Global COE Program "Photonics Integration-Core Electronics". The authors appreciate Dr. S. K. Singh (DRDO, Delhi) for the fabrication of 7.5 at. % BSFO films.

1) F. Kubel and H. Schmid: Acta Crystallor., Sect. B **46** (1990) 698.
2) C. Ederer and N. A. Spaldin: Nat. Mater. **3** (2004) 849.
3) W. Eerenstein, N. D. Mathur, and J. F. Scott: Nature **442** (2006) 759.
4) B. B. V. Aken, T. T. M. Palstra, A. Filippetti, and N. A. Spaldin: Nat. Mater. **3** (2004) 164.
5) S. K. Singh, K. Maruyama, and H. Ishiwara: J. Appl. Phys. **100** (2006) 064102.
6) X. Qi, J. Dho, R. Tomov, M. G. Blamire, and J. L. MacManus-Driscoll: Appl. Phys. Lett. **86** (2005) 062903.
7) S. K. Singh, K. Maruyama, and H. Ishiwara: Appl. Phys. Lett. **88** (2006) 262908.
8) S. K. Singh, K. Maruyama, and H. Ishiwara: Appl. Phys. Lett. **91** (2007) 112913.
9) H. Naganuma, J. Miura, and S. Okamura: Appl. Phys. Lett. **93** (2008) 052901.
10) S. K. Singh and H. Ishiwara: Jpn. J. Appl. Phys. **45** (2006) 3194.
11) Z. Y. Zhong, S. K. Singh, K. Maruyama, and H. Ishiwara: Jpn. J. Appl. Phys. **47** (2008) 2230.
12) S. Fujino, M. Murakami, V. Anbusathaiah, S. Lim, V. Nagarajan, C. J. Fennie, M. Wuttig, L. Salamanca-Rica, and I. Takeuchi: Appl. Phys. Lett. **92** (2008) 202904.
13) M. W. J. Prins, K. O. Grosse-Holz, J. F. M. Cilessen, and L. F. Feiner: J. Appl. Phys. **83** (1998) 888.
14) S. H. Hu, G. J. Hu, X. J. Meng, G. S. Wang, J. L. Sun, S. L. Guo, J. H. Chu, and N. Dai: J. Cryst. Growth **260** (2004) 109.
15) G. L. Yuan and S. W. Or: J. Appl. Phys. **100** (2006) 024109.
16) C. J. Cheng, D. Kan, S. H. Lim, W. R. McKenzie, P. R. Munroe, L. G. Salamanca-Riba, R. L. Withers, I. Takeuchi, and V. Nagarajan: Phys. Rev. B **80** (2009) 014109.
17) A. Rose: Phys. Rev. **97** (1955) 1538.
18) Z. Y. Zhong and H. Ishiwara: Appl. Phys. Lett. **95** (2009) 112902.